Time-differential perturbed-angular-correlation study of hyperfine interactions at ^{111}Cd in a $Li_{0.5}Fe_{2.5}O_4$ single crystal

Kichizo Asai and Takuya Okada
The Institute of Physical and Chemical Research (RIKEN), Wako-shi, Saitama 351-01, Japan

Tokio Yamadaya
Faculty of Literature and Science, Yokohama City University, Yokohama-shi, Kanagawa 232, Japan

Hisashi Sekizawa
Chiba Institute of Technology, Narashino-shi, Chiba 275, Japan
(Received 14 December 1987)

The time-differential perturbed angular correlation (TDPAC) of γ rays emitted from $^{111}Cd(\leftarrow{}^{111}In)$ on tetrahedral (A) sites in single-crystal $Li_{0.5}Fe_{2.5}O_4$ was measured at room temperature. Expressions for the anisotropy of TDPAC spectra under a hyperfine magnetic field combined with an electric field gradient (EFG) are given explicitly. A least-squares fitting of the data with these expressions reveals that $^{111}Cd^{2+}(A)$ experiences a supertransferred hyperfine magnetic field, H_{STHF}, of 112 kOe parallel to the net magnetization of the specimen and an axially symmetric EFG of 90×10^{13} esu. The observed H_{STHF} is seen to be the sum of the supertransferred ones from the $Fe^{3+}(B)$ ions on the nearest-neighbor B sites. The magnitude of the transferred field from each individual $Fe^{3+}(B)$ ion is estimated to be 13.3 or 11.0 kOe, depending on whether the intervening O^{2-} ion has $Li^{1+}(B)$ as its neighbor or not. The remarkably large EFG at $Cd^{2+}(A)$ observed in this ferrite is interpreted qualitatively as being caused by the presence of the weakly electronegative next-nearest $Li^{1+}(B)$ ions.

I. INTRODUCTION

Nuclei of nominally diamagnetic ions in magnetic oxides experience hyperfine magnetic fields transferred from the neighboring magnetic ions through the intervening oxygen ions.[1-19] This supertransferred hyperfine (STHF) magnetic field H_{STHF} has been widely studied in order to elucidate the electronic structure and the superexchange mechanism in magnetic oxides. In ferrimagnetic oxides with the spinel structure (spinel ferrites), H_{STHF} at $^{119}Sn^{4+}$ and $^{121}Sb^{5+}$, both occupying the octahedral (B) sites, have been systematically studied with the Mössbauer spectroscopy.[8-14] On the other hand, only a few studies have been made on H_{STHF} at the nuclei of diamagnetic ions occupying the tetrahedral (A) sites.[15,16]

We have been systematically investigating H_{STHF} at $^{11}Cd^{2+}$ in ferrimagnetic oxides with the spinel structure by means of the time-differential perturbed angular correlation (TDPAC) of the 171–245 keV cascade γ rays emitted from $^{111}Cd(\leftarrow{}^{111}In)$; the parent nuclei $^{111}In^{3+}$ occupy the A sites and the daughter nuclei $^{111}Cd^{2+}(A)$ feel H_{STHF} on these sites (the symbol in the parentheses denotes the cation site). In our previous studies on $M_xFe_{3-x}O_4$ (M = Ni or Co; $0.0\leq x\leq1.0$),[17-19] we found that H_{STHF} at $^{111}Cd^{2+}(A)$ is transferred from the magnetic ions on the nearest-neighbor B sites and can be regarded as the sum of the contributions of individual B site magnetic ions. The contribution of $Fe^{3+}(B)$ in these systems is 11.0 kOe in common, independent of the content x of M.[19]

In the present work, we studied H_{STHF} at $^{111}Cd^{2+}(A)$ in lithium ferrite. This ferrite is a completely inversed spinel $(Fe^{3+})[Li^{1+}_{0.5}Fe^{3+}_{1.5}]O_4$ and has a cubic structure belonging to $P4_32$ or $P4_12$, in which $Li^{1+}(B)$ and $Fe^{3+}(B)$ ions form an ionic order in the B sites.[20-22] It should be noted that this ferrite has the highest Curie temperature (T_C = 943 K) among all the spinel ferrites[23] although one-fourth of the B sites are occupied by diamagnetic ions $Li^{1+}(B)$. This fact suggests that the superexchange interaction between $Fe^{3+}(A)$ and $Fe^{3+}(B)$ via O^{2-} is considerably stronger in $Li_{0.5}Fe_{2.5}O_4$ than in other spinel ferrites. One of our aims of this study is to find the origin of such a strong superexchange interaction in this ferrite. A comparison of the STHF interaction in $Cd^{2+}(A)$—O^{2-}—$Fe^{3+}(B)$ bond in this ferrite with those in other ferrites is expected to provide valuable information on this problem.

The tetrahedral (A) sites of lithium ferrite can be classified into four kinds of equivalent sites, each of which has a trigonal axis parallel to one of $\langle111\rangle$ as shown in Fig. 1. Because of the trigonal symmetry of the A sites in this ferrite, $^{111}Cd^{2+}(A)$ can experience an axially symmetric electric field gradient (EFG) in addition to H_{STHF}. When the magnetic field H_{STHF} and EFG coexist in a ferro or a ferrimagnet, there are unavoidable ambiguities in the analysis of the TDPAC spectra for polycrystalline samples, as will be shown in Sec. III. In the present study, we measure TDPAC spectra for both poly- and single-crystal $Li_{0.5}Fe_{2.5}O_4$ and prove that experiments using single crystals are essential to obtain unambi-

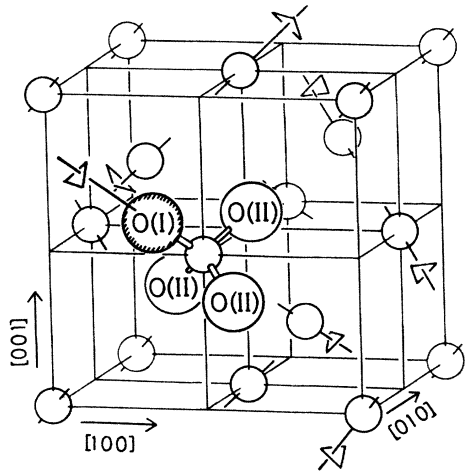

FIG. 1. Directions of the trigonal axes of the tetrahedral (A) sites and the configuration of oxygen ions around one of the A sites in $Li_{0.5}Fe_{2.5}O_4$.

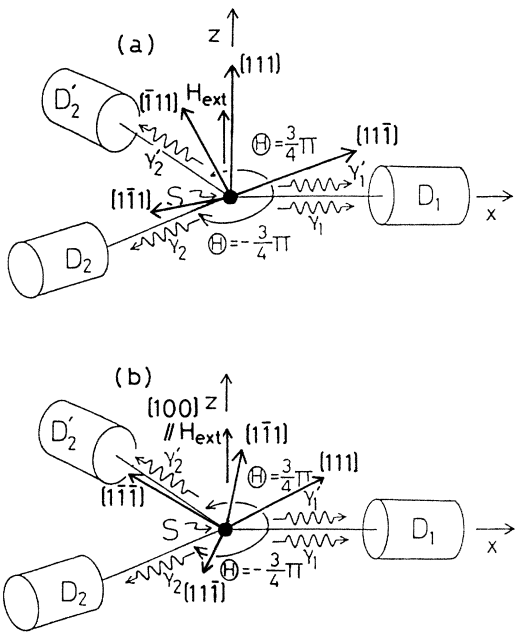

FIG. 2. Geometries of the single crystal, detectors, and the externally applied magnetic field: (a) $[111]\|\mathbf{H}_{ext}$ and $[11\bar{1}]$ in the x-z plane, and (b) $[100]\|\mathbf{H}_{ext}$ and [111] in the x-z plane.

guous results.

This paper consists of three major parts. The sample preparation, the experimental procedure, and the results are described in Sec. II. In Sec. III expressions for the anisotropy of TDPAC spectra under a hyperfine magnetic field combined with an EFG are derived, and the observed spectra are analyzed by these expressions. In Sec. IV the effect of $Li^{1+}(B)$ ions on the covalencies of their neighboring $Cd^{2+}(A)$—O^{2-}—$Fe^{3+}(B)$ bonds, and consequently on the STHF interactions in them, is discussed.

II. EXPERIMENTAL PROCEDURE AND RESULTS

Polycrystalline $Li_{0.5}Fe_{2.5}O_4$ samples were prepared by calcination of a mixture of Li_2CO_3 and α-Fe_2O_3 in the appropriate proportion at 1000 °C in O_2 gas flow for about 10 h. Single crystals of $Li_{0.5}Fe_{2.5}O_4$ were grown in a flux system PbO-B_2O_3 by a method similar to the ones described in Refs. 24 and 25. An appropriate mixture of Li_2CO_3, α-Fe_2O_3, B_2O_3, and PbO in a 50-cm^3 platinum crucible was heated up to 1050 °C. The content was stirred and kept at that temperature for 2 h to be homogenized, then cooled to 1010 °C, again held at this temperature for 20 h, cooled down to 400 °C at a rate of about 2 °C/h, and finally furnace cooled down to room temperature. The crystals were taken out of the flux by immersing the crucible in hot dilute HNO_3. The crystals thus grown were in an octahedral form with edge dimensions of about 3 mm.

The "carrier-free" parent nuclide ^{111}In was diffused into the polycrystals at 1100 °C for 2 h and into the single crystals at 1150 °C for 2 days both in O_2 gas flow. The poly or single crystals containing about 120 μCi of ^{111}In were subjected to TDPAC measurement at room temperature. An external magnetic field H_{ext} of 10 kOe was applied perpendicularly to the detectors plane to polarize the magnetization of the specimens completely in this direction. The measurements on the single crystals were made in two different geometries as shown in Fig. 2. In the first geometry, [111] was parallel to $\mathbf{H}_{ext}$ ($\|z$) and $[11\bar{1}]$ in the x-z plane, and in the second, [100] was parallel to $\mathbf{H}_{ext}$ and [111] in the x-z plane. Here, the x axis was defined by the direction of the first γ ray detector. Time spectra $N(\Theta,t)$ of the 171–245 keV γ-γ cascade emitted from ^{111}Cd were taken using a conventional fast-slow setup with NaI (Tl) detectors at $\Theta=\pm 3\pi/4$.[18] Here Θ and t denote the angle and the time interval between the cascade γ rays, respectively. The normalized anisotropy $R(t)$ of the angular correlation was defined by

$$R(t)=\frac{[N(-3\pi/4,t)-N(+3\pi/4,t)]}{[N(-3\pi/4,t)+N(+3\pi/4,t)]}\ , \tag{1}$$

after the accidental coincident counts being subtracted from the time spectra.

The normalized anisotropy $R(t)$ for polycrystalline $Li_{0.5}Fe_{2.5}O_4$ at room temperature and its Fourier spectrum are shown in Figs. 3(a) and 3(b); respectively. As can be seen, the Fourier spectrum has a considerably broad intensity distribution around 3.5×10^8 rad/s and seems to have some structure.

The normalized anisotropies $R(t)$ for single-crystal $Li_{0.5}Fe_{2.5}O_4$ are shown in Figs. 4(a) and 4(b); 4(a) in the first geometry ($[111]\|\mathbf{H}_{ext}$), and 4(b) in the second geometry ($[100]\|\mathbf{H}_{ext}$). There can be seen a remarkable difference between these two spectra. As will be explained in Sec. III, this fact shows that an appreciable magnitude of EFG is acting on $^{111}Cd^{2+}(A)$ in addition to the hyperfine magnetic field H_{hyp}, which is perpendicular to the detectors plane. The external magnetic field H_{ext} is included in H_{hyp}.

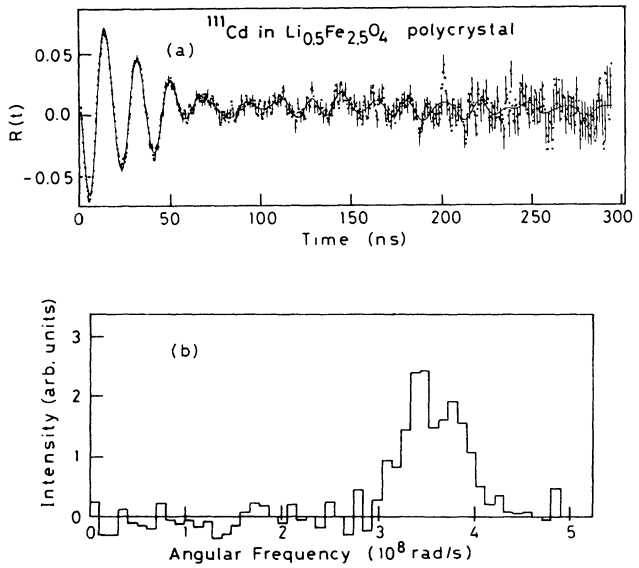

FIG. 3. (a) The normalized anisotropy $R(t)$ of the angular correlation of γ rays emitted from ^{111}Cd($\leftarrow^{111}$In) in polycrystalline $Li_{0.5}Fe_{2.5}O_4$ at room temperature. The solid curve is the fitted one with the Fourier spectrum shown (b). (b) The Fourier spectrum of $R(t)$.

III. ANALYSIS OF THE TDPAC SPECTRA

A. Expressions for the anisotropy of TDPAC spectra for ^{111}Cd($\leftarrow^{111}$In) under H_{hyp} combined with an EFG

We derive expressions for the anisotropy of TDPAC spectra for ^{111}Cd($\leftarrow^{111}$In) in a single crystal with a hyperfine magnetic field H_{hyp} perpendicular to the detectors plane combined with an axially symmetric EFG. We take the $A_{k_1k_2}$ terms with $k_1=2$ and $k_2=2$ or 4 into account, because only the angular correlation coefficients $A_{k_1k_2}$ with these k_i have appreciable values in the case of ^{111}Cd($\leftarrow^{111}$In) $\frac{7}{2}+\rightarrow\frac{5}{2}+\rightarrow\frac{1}{2}+$ cascade.[26] Here, k_i is the multiplicity of the ith radiation.

The perturbed angular correlation can be written in the form[27]

$$W(\mathbf{k}_1,\mathbf{k}_2,t)=\sum_{\substack{k_1,k_2\\N_1,N_2}} A_{k_1k_2}G_{k_1k_2}^{N_1N_2}(t)\times[(2k_1+1)(2k_2+1)]^{-1/2}\times Y_{k_1}^{N_1}(\theta_1,\phi_1)Y_{k_2}^{N_2}(\theta_2,\phi_2)\ . \quad (2)$$

Here, θ_i and ϕ_i are the polar angles of the propagation direction $\mathbf{k}_i$ of the ith radiation, $Y_{k_i}^{N_i}(\theta_i,\phi_i)$ the spherical harmonics, and $G_{k_1k_2}^{N_1N_2}(t)$ the perturbation factor.

We choose a coordinate system with the quantization axis z parallel to the magnetic field, and the axis x to the propagation direction of the first radiation. We then specify the principal axis z' of the axially symmetric EFG by the polar angles β and γ (see Fig. 5). The perturbation factor can now be written in the form[28]

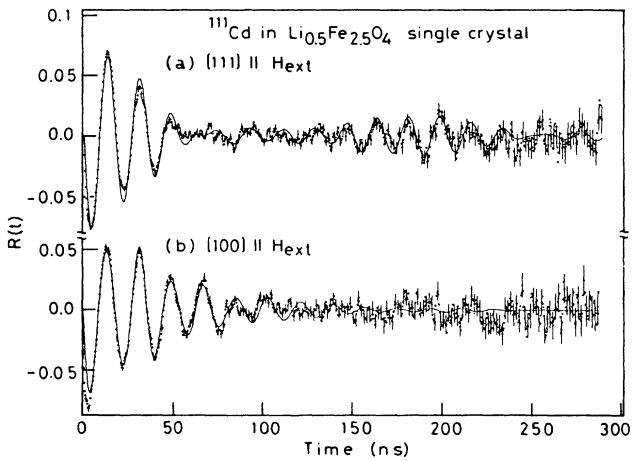

FIG. 4. The normalized anisotropies $R(t)$ of the angular correlations of γ rays emitted from ^{111}Cd($\leftarrow^{111}$In) in single-crystal $Li_{0.5}Fe_{2.5}O_4$ at room temperature. The solid curves are the fitted ones with the Fourier spectra shown in Fig. 6: (a) $[111]\|\mathbf{H}_{ext}$ and $[11\bar{1}]$ in the x-z plane, and (b) $[100]\|\mathbf{H}_{ext}$ and $[111]$ in the x-z plane.

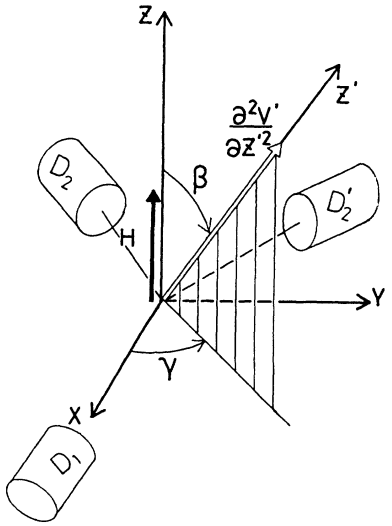

FIG. 5. Directions of the magnetic field and the principal axis of the axially symmetric electric field gradient at ^{111}Cd. The detector D_1 for γ_1 and γ_1' is on the x axis ($\theta_1=\pi/2,\phi_1=0$), and those, D_2 for γ_2 and D_2' for γ_2', are in the x-y plane ($\theta_2=\theta_2'=\pi/2$) with $\phi_2=-3\pi/4$ and $\phi_2'=+3\pi/4$.

$$G_{k_1k_2}^{N_1N_2}(t)=\sum_{\substack{m_a,m_b,\\ n,n'}}(-1)^{2I+m_a+m_b}[(2k_1+1)(2k_2+1)]^{1/2}\begin{bmatrix} I & I & k_1 \\ m_a' & -m_a & N_1\end{bmatrix}\begin{bmatrix} I & I & k_2 \\ m_b' & -m_b & N_2\end{bmatrix}$$
$$\times\langle n\mid m_b\rangle^*\langle n\mid m_a\rangle\langle n'\mid m_b'\rangle\langle n'\mid m_a'\rangle^*\exp[(-i/\hbar)(E_n-E_n')t]\exp[i\gamma(N_1-N_2)]\ . \tag{3}$$

Here,

$$\begin{bmatrix} I & I & k_1 \\ m_a' & -m_a & N_1\end{bmatrix}$$

is the Wigner 3-j symbol, $\mid m_a\rangle$ the state defined by the magnetic quantum number m_a, and $\mid n\rangle$ and E_n are the energy eigenstate and eigenvalue, respectively, of the Hamiltonian for $\gamma=0$ (i.e., the principal axis z' of the EFG being in the x-z plane). The matrix elements $\langle n\mid m\rangle$ can be taken to be real and are functions of the Larmor frequency ω_L, the electric quadrupolar frequency ω_Q, and the angle β.

The observed time spectra $N(\Theta,t)$ are expressed in terms of $W(\mathbf{k}_1,\mathbf{k}_2,t)$ as $N(\Theta,t)=W(\mathbf{k}_1,\mathbf{k}_2,t)\exp(-t/\tau_N)$, where τ_N is the lifetime of the intermediate state ($I=\frac{5}{2}$) of ^{111}Cd. Then, we calculate the normalized anisotropy $R(t)$ of the time spectra $N(\Theta,t)$ defined by Eq. (1). Because of the angular dependences of the spherical harmonics, only $G_{k_1k_2}^{N_1N_2}(t)$ terms with $\mid N_1\mid=0$ or 2, and $\mid N_2\mid=2$ contribute to $R(t)$ in our coordinate system: $\theta_1=\theta_2=\pi/2$, $\phi_1=0$, and $\phi_2=+3\pi/4$ or $-3\pi/4$. By inserting Eq. (3) into Eq. (2) and using the relation $G_{k_1k_2}^{-N_1-N_2}(t)=[G_{k_1k_2}^{N_1N_2}(t)]^*$, $R_{\Delta N}(t)$ arising from the $G_{k_1k_2}^{N_1N_2}(t)$ terms with $\mid N_1-N_2\mid=\Delta N$ are written explicitly:

$$R_0(t)=\frac{15}{4}A_{22}\sum_{\substack{m_a,m_b\\ n,n'}}(-1)^{2I+m_a+m_b}\begin{bmatrix} I & I & 2 \\ m_a' & -m_a & 2\end{bmatrix}\left[\begin{bmatrix} I & I & 2 \\ m_b' & -m_b & 2\end{bmatrix}-\frac{\sqrt{3}}{2}\frac{A_{24}}{A_{22}}\begin{bmatrix} I & I & 4 \\ m_b' & -m_b & 2\end{bmatrix}\right]$$
$$\times\langle n\mid m_b\rangle^*\langle n\mid m_a\rangle\langle n'\mid m_b'\rangle\langle n'\mid m_a'\rangle^*\sin[(1/\hbar)(E_n-E_n')t]\ , \tag{4a}$$

$$R_2(t)=-\frac{5}{2}\left[\frac{3}{2}\right]^{1/2}A_{22}\sum_{\substack{m_a,m_b\\ n,n'}}(-1)^{2I+m_a+m_b}\begin{bmatrix} I & I & 2 \\ m_a' & -m_a & 0\end{bmatrix}\left[\begin{bmatrix} I & I & 2 \\ m_b' & -m_b & 2\end{bmatrix}-\frac{\sqrt{3}}{2}\frac{A_{24}}{A_{22}}\begin{bmatrix} I & I & 4 \\ m_b' & -m_b & 2\end{bmatrix}\right]$$
$$\times\langle n\mid m_b\rangle^*\langle n\mid m_a\rangle\langle n'\mid m_b'\rangle\langle n'\mid m_a'\rangle^*\sin[(1/\hbar)(E_n-E_n')t+2\gamma]\ , \tag{4b}$$

$$R_4(t)=\frac{15}{4}A_{22}\sum_{\substack{m_a,m_b,\\ n,n'}}(-1)^{2I+m_a+m_b}\begin{bmatrix} I & I & 2 \\ m_a' & -m_a & -2\end{bmatrix}\left[\begin{bmatrix} I & I & 2 \\ m_b' & -m_b & 2\end{bmatrix}-\frac{\sqrt{3}}{2}\frac{A_{24}}{A_{22}}\begin{bmatrix} I & I & 4 \\ m_b' & -m_b & 2\end{bmatrix}\right]$$
$$\times\langle n\mid m_b\rangle^*\langle n\mid m_a\rangle\langle n'\mid m_b'\rangle\langle n'\mid m_a'\rangle^*\sin[(1/\hbar)(E_n-E_n')t+4\gamma]\ . \tag{4c}$$

When the hyperfine magnetic interaction is predominant over the electric quadrupolar one, the magnetic sublevels $\mid m\rangle$ are approximately the eigenstates of the Hamiltonian, and only the term $R_0(t)$ has an appreciable amplitude because of the orthogonality relation of the 3-j symbols. In this limit ($\omega_Q\ll\omega_L$), $R_0(t)$ is written as

$$R_0(t)=\tfrac{15}{4}A_{22}\sum_n\begin{bmatrix} I & I & 2 \\ n' & -n & 2\end{bmatrix}\left[\begin{bmatrix} I & I & 2 \\ n' & -n & 2\end{bmatrix}-\frac{\sqrt{3}}{2}\frac{A_{24}}{A_{22}}\begin{bmatrix} I & I & 4 \\ n' & -n & 2\end{bmatrix}\right]\sin\left[\left[2\omega_L+6(n+n')\omega_Q\frac{3\cos^2\beta-1}{2}\right]t\right]\ , \tag{5}$$

i.e., four Fourier components appear symmetrically around $\omega=2\omega_L$ with an interval of $6\omega_Q(3\cos^2\beta-1)$. The summed amplitude of these components is $(3/4)A_{22}$, the value previously derived for the case in which only the hyperfine magnetic field $H_{\rm hyp}$ exists.[18]

The anisotropy $R(t)$ for a polycrystal is derived by averaging $R(t)$ over all directions. It can be shown that the averages of $R_{\Delta N}(t)$ with $\Delta N\neq0$ are zero and that the average of $R_0(t)$ in Eq. (4a) has distributed Fourier components due to the distribution of the angle β.

Thus, an important conclusion is derived as follows: Given an observed distribution of the Fourier components of $R(t)$ for a polycrystalline sample, it is impossible in general to determine whether the distribution is caused by a distribution of $H_{\rm hyp}$, or otherwise caused by an EFG coexisting with $H_{\rm hyp}$.

B. TDPAC spectra for ^{111}Cd($\leftarrow^{111}$In) in single-crystal $Li_{0.5}Fe_{2.5}O_4$

In $Li_{0.5}Fe_{2.5}O_4$, tetrahedral (A) sites are classified into four kinds; each of which has a trigonal axis parallel to one of $\langle 111 \rangle$ (see Fig. 1). The observed anisotropy $R_{obs}(t)$ for the single crystal is an average of $R(t)$ for these four kinds of A sites. In the first geometry where H_{hyp} is parallel to [111] [see Fig. 2(a)], the principal axis of EFG for one particular kind of site is parallel to H_{hyp} ($\beta=0°$), and those for the remaining three are oriented symmetrically around H_{hyp} with $\beta=70.5°$, and $\gamma=120°\times n$ ($n=0$, 1, or 2). The anisotropy $R(t)$ for the former kind of sites contains only $R_0(t)$ term because $\beta=0°$. The average of $R(t)$ for the latter three also contains only $R_0(t)$ because the terms $R_{\Delta N}(t)$ with $\Delta N=2$ or 4 for these sites cancel out mutually due to the phase in the last factor in Eqs. (4b) or (4c). Thus the quantity $R_{obs}(t)$ for this geometry can be written as

$$R_{obs}(t)=(1/4)R_0(t)_{\beta=0°}+(3/4)R_0(t)_{\beta=70.5°}, \quad (6)$$

which does not depend on γ.

In the second geometry where H_{hyp} is parallel to [100] [see Fig. 2(b)], the principal axes of EFG for all the four kinds of sites are oriented symmetrically around H_{hyp} with $\beta=54.7°$ and $\gamma=90°\times n$ ($n=0$, 1, 2, or 3). In this geometry, the average of $R(t)$ for these four kinds of sites contains not only the $R_0(t)$ term but also $R_4(t)$. These terms are common to all the sites and the quantity $R_{obs}(t)$ can be written as

$$R_{obs}(t)=R_0(t)_{\beta=54.7°}+R_4(t)_{\beta=54.7°,\gamma=0°}. \quad (7)$$

The observed spectra in Figs. 4(a) and 4(b) were fitted with $R_{obs}(t)$ in Eqs. (6) and (7), respectively. The ratio of the effective angular correlation coefficients $(A_{24}/A_{22})_{eff}$ corrected for the finite solid angles of the detectors was calculated to be 1.1 for our experimental setup.[26,29] It was assumed that each Fourier component in Eqs. (4a) and (4c) has a distribution of the Lorentzian shape. The fitting parameters for each spectrum were ω_L, ω_Q, and the width of the distribution. The fitted curves and their Fourier spectra are shown in Figs. 4 and 6, respectively. The observed spectra for both the geometries can be reproduced well with a common set of ω_L and ω_Q, but the widths of the Fourier components are considerably large, and different from each other. The derived H_{hyp} is 122 kOe parallel to the B site magnetization, and the magnitude of EFG is 90×10^{13} esu.

It was found in the fitting procedure that the amplitude of the term $R_4(t)$ in Eq. (7) is only one-thousandth of $R_0(t)$ in the present case with $\gamma=0°$ and does not exceed a few percent for any value of γ. Thus, the spectrum is almost unchanged by a rotation of the crystal around the z axis even in the second geometry.

IV. DISCUSSION

The TDPAC spectra for single-crystal $Li_{0.5}Fe_{2.5}O_4$ can be analyzed with a set of a hyperfine magnetic field and an axially symmetric EFG. In the analysis, the directions

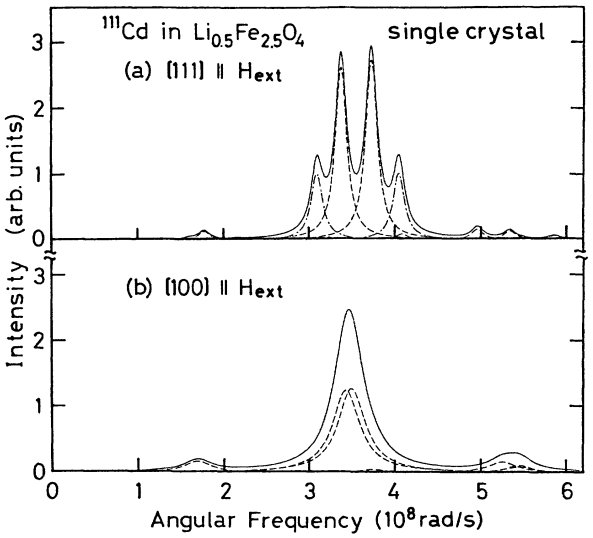

FIG. 6. Fourier spectra of $R(t)$ for single-crystal $Li_{0.5}Fe_{2.5}O_4$ at room temperature. Dotted lines represent individual Fourier components and solid lines the total of them: (a) [111]∥$\mathbf{H}_{ext}$ and [11$\bar{1}$] in the x-z plane. – – – for $(3/4)R_0(t)_{\beta=70.5°}$, and –·– for $(1/4)R_0(t)_{\beta=0°}$. (b) [100]∥$\mathbf{H}_{ext}$ and [111] in the x-z plane.

of the principal axes of EFG are assumed to be parallel to the ones expected from the crystallographic study of the ordered $Li_{0.5}Fe_{2.5}O_4$.[20–22] The satisfactory agreement between the observation and the analysis means that the ionic order of $Fe^{3+}(B)$ and $Li^{1+}(B)$ is kept well around $Cd^{2+}(A)$. The fairly large widths of the Fourier components are ascribed to the after effects of the EC decay of ^{111}In$\rightarrow^{111}$Cd. It is known that in insulators both the magnitude and the orientation of EFG at $^{111}Cd^{2+}(\leftarrow^{111}In)$ observed by TDPAC are considerably distributed around those for the ground state Cd^{2+} ions by the after effects of the preceding EC decay.[30–32]

The field H_{STHF} in $Li_{0.5}Fe_{2.5}O_4$ derived from the observed hyperfine magnetic field H_{hyp} is 112 kOe, which is parallel to the B site magnetization as in other spinel ferrites. Figure 7 shows the ionic configurations in $Li_{0.5}Fe_{2.5}O_4$. As shown in Fig. 7(a), $Cd^{2+}(A)$ is surrounded by four O^{2-} ions of two kinds denoted by O^{2-}(I) and O^{2-} (II). The trigonal axis lies along $Cd^{2+}(A)$—O^{2-}(I) bond. As can be seen in Figs. 7(b) and 7(c), three $Fe^{3+}(B)$ ions are linked to the $Cd^{2+}(A)$ through O^{2-}(I) ion, but on the other hand, two $Fe^{3+}(B)$ and one $Li^{1+}(B)$ ion are linked through O^{2-}(II). Since H_{STHF} at A site ion can be regarded as a sum of the STHF fields from the nearest-neighbor B site magnetic ions through O^{2-}(I) or O^{2-}(II) in this structure,[15,18,19] the magnitude of the field from each $Fe^{3+}(B)$ ion [denoted by $h(\leftarrow Fe^{3+})$] is 12.4 kOe on average.

The above value is more than 10% larger than the one (11.0 kOe) in $M_xFe_{3-x}O_4$ (M=Ni or Co) system.[19] It should be noted that the value in the latter system does not depend on the kind of ion M and its content x. The lattice constants, the oxygen parameters (u parameters),[33] and other physical parameters of MFe_2O_4 (M=Fe, Co,

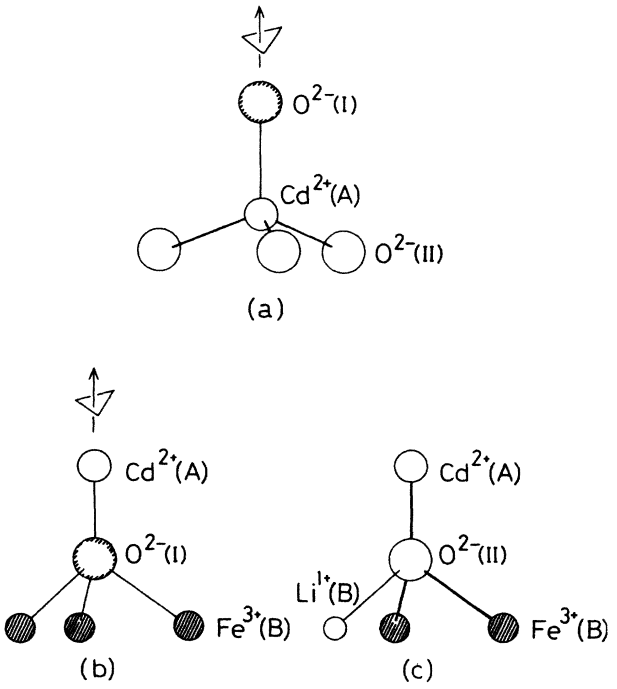

FIG. 7. Local ionic configurations in $Li_{0.5}Fe_{2.5}O_4$: (a) O^{2-} ions around $Cd^{2+}(A)$. The trigonal axis lies along $Cd^{2+}(A)$—$O^{2-}(I)$ bond. (b) Cations around $O^{2-}(I)$ ions. (c) Cations around $O^{2-}(II)$ ions.

TABLE I. The lattice constants a, the oxygen parameters u, and the Curie temperatures T_C of spinel ferrites, and the supertransferred hyperfine magnetic fields $h(\leftarrow Fe^{3+})$ at $^{111}Cd^{2+}(A)$ from a single $Fe^{3+}(B)$ ion on the nearest B site in them.

Material	a[a,b] (A)	u[b]	T_C[a] (K)	$h(\leftarrow Fe^{3+})$[b] (kOe)
Fe_3O_4	8.39	0.379[a]	858	11.0[c]
$CoFe_2O_4$	8.38	0.3818[d]	793	11.0[c]
$NiFe_2O_4$	8.34	0.3822[d]	858	11.0[c]
$Li_{0.5}Fe_{2.5}O_4$	8.33[e]	0.382[a]	943	12.4[f]

[a]Reference 23.
[b]At room temperature.
[c]Derived from the variation of STHF fields at $Cd^{2+}(A)$ with x in $M_xFe_{3-x}O_4$ (M = Ni or Co) system. Possible error is ±0.2 kOe. See Ref. 19.
[d]S. Krupička and P. Novák, in *Ferromagnetic Materials*, edited by E. P. Wohlfarth (North-Holland, Amsterdam, 1982), Vol. 3, Chap. 4, pp. 189–304.
[e]The value is 8.337 in Ref. 22.
[f]Present result.

and Ni) and $Li_{0.5}Fe_{2.5}O_4$ are tabulated in Table I. As can be seen, the lattice constant of MFe_2O_4 decreases appreciably along with a slight increase of the u parameter in sequence of M = Fe, Co, and Ni. Furthermore, both the lattice constant and the u parameter of $NiFe_2O_4$ are almost the same with those of $Li_{0.5}Fe_{2.5}O_4$. This fact means that the large value of $h(\leftarrow Fe^{3+})$ in $Li_{0.5}Fe_{2.5}O_4$ as compared with those in MFe_2O_4 system can be explained neither by the small lattice constant nor by the u parameter of $Li_{0.5}Fe_{2.5}O_4$, but should be attributed to the presence of Li^{1+} ions.

The STHF interaction between $Cd^{2+}(A)$ and $Fe^{3+}(B)$ can be divided into two processes[1–6]: The first is the polarization of the ligand electrons of O^{2-} ions by the $3d$ electrons of $Fe^{3+}(B)$ ions, and the second is the polarization of s electrons of $Cd^{2+}(A)$ ions by these ligand electrons. These two processes are caused by the overlap distortion and the transfer mechanisms in the relevant chemical bonds [$Fe^{3+}(B)$—O^{2-} for the first process, O^{2-}—$Cd^{2+}(A)$ for the second], and it is known that the magnitude of the total STHF interaction increases with an increase of the covalency of either bond.[1–6] Now, we consider the effect of $Li^{1+}(B)$ ions on the covalencies of the neighboring $Cd^{2+}(A)$—O^{2-}(II) and $Fe^{3+}(B)$—O^{2-}(II) bonds in the following.

The electronegativities[34] of the $3d$ transition metal ions and the Li^{1+} ion are listed in Table II. As can be seen in the table, the electronegativities of $3d$ transition metal ions are nearly equal to each other, but that of the Li^{1+} ion is remarkably smaller than these. It will occur as a result of this smaller electronegativity of $Li^{1+}(B)$ that the ligand electrons of O^{2-}(II) are polarized towards the $Cd^{2+}(A)$ and the two $Fe^{3+}(B)$ ions to some extent since the electrons are less attracted towards the $Li^{1+}(B)$. Then, the covalencies of the chemical bonds $Cd^{2+}(A)$—O^{2-}(II) and $Fe^{3+}(B)$—O^{2-}(II) are expected to be larger than the corresponding bonds with no adjacent $Li^{1+}(B)$ in this or in other ferrites.

This influence of the $Li^{1+}(B)$ ions on the neighboring bonds is expected also by the electrostatic valence principle first proposed by Pauling[35] and extended later by other workers.[36,37] The meaning of the original principle is as follows. In solids, the strength of the valence bond between a cation and an anion (bond strength) is defined as the valence of the cation divided by its coordination number. The sum of such strengths around each anion generally coincides with the valence of the anion. This original principle holds in most solids at least approximately. Then, the extended principle postulates the following. When the original principle does not hold exactly as in $Li_{0.5}Fe_{2.5}O_4$, the individual bond strengths in the original principle are modified in such a way that their sum around each ion approaches the valence of the ion. The bond strengths thus modified are positively correlated to the covalencies of the bonds.[37] Applying this extended principle to the present case of $Li_{0.5}Fe_{2.5}O_4$, the bond strengths or the covalencies of $Cd^{2+}(A)$—O^{2-}(II) and $Fe^{3+}(A)$—O^{2-}(II) bonds are enhanced by the presence of the neighboring $Li^{1+}(B)$ because of the small bond

TABLE II. The electronegativities of Li and some $3d$ transition metal ions (Ref. 34).

Ion	Li^{1+}	Fe^{2+}	Fe^{3+}	Co^{2+}	Ni^{2+}
Electronegativity	0.95	1.7	1.8	1.7	1.7

strengths of $Li^{1+}(B)$—O^{2-}(II) bonds.

A large value of $h(\leftarrow Fe^{3+})$ through O^{2-}(II) is expected on the basis of the above discussion. On the other hand, the value of $h(\leftarrow Fe^{3+})$ through O^{2-}(I) is expected to be not much different from those in $M_xFe_{3-x}O_4$ (M = Ni or Co) system as will be discussed later. If we assume that $h(\leftarrow Fe^{3+})$ through O^{2-}(I) is 11.0 kOe as in $M_xFe_{3-x}O_4$, $h(\leftarrow Fe^{3+})$ through O^{2-}(II) must be 13.3 kOe, about 20% larger than the former.

The EFG at $Cd^{2+}(A)$ in $Li_{0.5}Fe_{2.5}O_4$ is remarkably large. This large and axially symmetric EFG is explained as a result of the difference of the covalencies between one $Cd^{2+}(A)$—O^{2-}(I) and three $Cd^{2+}(A)$—O^{2-}(II) bonds around $Cd^{2+}(A)$ in this crystal [see Fig. 7(a)]. It should be noted that no appreciable EFG is observed at $Cd^{2+}(A)$ in $M_xFe_{3-x}O_4$ system although the nearest-neighbor B sites around $Cd^{2+}(A)$ are occupied randomly by Fe and M ions and thus the point symmetry at $Cd^{2+}(A)$ is lower than cubic. This fact, along with the constant value of $h(\leftarrow Fe^{3+})$ in the system, means that the effects of Fe(B) and $M(B)$ ions on the covalencies (and consequently on the STHF interactions) of the neighboring bonds are not different from each other, as expected also from the similar magnitude of the electronegativities of these 3d transition metal ions.

The STHF and superexchange interactions have a noticeable similarity[5,6]; both increase with increases of the covalencies of the relevant chemical bonds. The covalency of $Fe^{3+}(A)$—O^{2-}(II) bonds should be enhanced by the presence of the neighboring $Li^{1+}(B)$ ions. Then, a large magnitude of the superexchange interaction is expected in $Fe^{3+}(A)$—O^{2-}(II)—$Fe^{3+}(B)$ bond, resulting in the high T_C of $Li_{0.5}Fe_{2.5}O_4$, the highest among all the spinel ferrites.

V. CONCLUSION

The supertransferred hyperfine magnetic field H_{STHF} and the electric field gradient (EFG) at Cd^{2+} on the A sites in $Li_{0.5}Fe_{2.5}O_4$ were obtained by means of TDPAC of γ rays emitted from $^{111}Cd(\leftarrow{}^{111}In)$ in the single crystals. The value of the STHF magnetic field transferred from a single $Fe^{3+}(B)$, $h(\leftarrow Fe^{3+})$, was found to be 12.4 kOe on average, which is 10% larger than that in $M_xFe_{3-x}O_4$ (M = Co or Ni) system. This large value was accounted for through an effect of $Li^{1+}(B)$ ions on the STHF interactions in their adjacent $Cd^{2+}(A)$—O^{2-}—$Fe^{3+}(B)$ bonds. The covalencies of $Cd^{2+}(A)$—O^{2-} and $Fe^{3+}(B)$—O^{2-} bonds are enhanced when these bonds share O^{2-} ion with $Li^{1+}(B)$ ion because the electronegativity of $Li^{1+}(B)$ is considerably smaller than those of 3d transition metal ions. It was estimated that $h(\leftarrow Fe^{3+})$ through the oxygen ion O^{2-}(II) which has one $Li^{1+}(B)$ on its neighbor site is 13.3 kOe, and the one through the oxygen O^{2-}(I) with no adjacent $Li^{1+}(B)$ is 11.0 kOe.

The remarkably large EFG observed at $Cd^{2+}(A)$ in this ferrite is accounted for by the difference between the covalencies of one $Cd^{2+}(A)$—O^{2-}(I) and three $Cd^{2+}(A)$—O^{2-}(II) bonds around $Cd^{2+}(A)$. The superexchange interactions between $Fe^{3+}(A)$ and $Fe^{3+}(B)$ ions through O^{2-}(II) ions in this ferrite are expected to be large by the same mechanism for the large STHF interactions through O^{2-}(II). These large superexchange interactions in $Li_{0.5}Fe_{2.5}O_4$ are considered to be an origin of the high Curie temperature of this ferrite.

ACKNOWLEDGMENTS

The authors wish to express their hearty thanks to Dr. F. Ambe and Dr. S. Ambe for their advice and stimulating discussions throughout this work. We also gratefully acknowledge Professor K. Kohn of Waseda University for his many valuable suggestions, Dr. N. Sakai and Dr. N. Shiotani for their critical readings of the manuscript, and Dr. A. Hashizume for his technical advice.

[1]N. L. Huang, R. Orbach, E. Šimánek, J. Owen, and D. R. Taylor, Phys. Rev. **156**, 383 (1967).

[2]J. Owen and D. R. Taylor, J. Appl. Phys. **39**, 791 (1968).

[3]E. Šimánek and Z. Šroubek, in *Electron Paramagnetic Resonance*, edited by S. Geschwind (Plenum, New York, 1972), Chap. 8, p. 535.

[4]D. R. Taylor, J. Owen, and B. M. Wanklyn, J. Phys. C **6**, 2592 (1973).

[5]C. Boekema, F. van der Woude, and G. A. Sawatzky, Int. J. Magn. **3**, 341 (1972).

[6]G. A. Sawatzky and F. van der Woude, J. Phys. (Paris) Colloq. **35**, C6-47 (1974).

[7]R. L. Streever and G. A. Uriano, Phys. Rev. **139**, A305 (1965).

[8]G. V. Novikov, V. A. Trukhtanov, S. I. Yushchuk, and N. A. Grigoryan, Fiz. Tverd. Tela (Leningrad) **9**, 1840 (1968) [Sov. Phys.—Solid State **9**, 2350 (1968)].

[9]I. S. Lyubutin, T. Ohya, T. V. Dmitrieva, and K. Ôno, J. Phys. Soc. Jpn. **36**, 1006 (1974).

[10]G. V. Novikov, V. A. Trukhtanov, L. Cser, S. I. Yushchuk, and V. I. Gol'danskiĭ, Zh. Eksp. Teor. Fiz. **56**, 743 (1969) [Sov. Phys.—JETP **29**, 403 (1969)].

[11]H. Sekizawa, T. Okada, and F. Ambe, Physica **86-88B**, 963 (1977).

[12]S. L. Ruby, B. J. Evans, and S. S. Hafner, Solid State Commun. **6**, 277 (1968).

[13]B. J. Evans and L. J. Swartzendruber, Phys. Rev. B **6**, 223 (1972).

[14]B. J. Evans and L. J. Swartzendruber, in *Magnetism and Magnetic Materials (Boston, 1973)*, Proceedings of the 19th Annual Conference on Magnetism and Magnetic Materials, AIP Conf. Proc. No. 18, edited by C. D. Graham and J. J. Rhyne (AIP, New York, 1974), p. 518.

[15]Y. Miyahara and S. Iida, J. Phys. Soc. Jpn. **37**, 1248 (1974).

[16]V. D. Doroshev, V. A. Klochan, N. M. Kovtun, and V. N. Seleznev, Phys. Status Solidi A **26**, 77 (1974).

[17]K. Asai, T. Okada, F. Ambe, S. Ambe, and H. Sekizawa, in *Condensed Matter Studies by Nuclear Methods (Zakopane, 1985)*, Proceedings of the 20th Winter School on Physics,

edited by J. J. Bara, K. Ruebenbauer, and Z. Stachura (Institute of Nuclear Physics and Jagiellonian University, Cracow, 1985), Vol. 2, p. 400.

[18]K. Asai, T. Okada, and H. Sekizawa, J. Phys. Soc. Jpn. **54**, 4325 (1985).

[19]K. Asai, T. Okada, and H. Sekizawa (unpublished). A preliminary result is in the article by K. Asai, T. Okada, and H. Sekizawa, in Hyperfine Int. **34**, 435 (1987).

[20]P. B. Braun, Nature (London) **170**, 1123 (1952).

[21]E. W. Gorter, Philips Res. Rep. **9**, 295 (1954).

[22]M. Schieber, J. Inorg. Nucl. Chem. **26**, 1363 (1964).

[23]J. Smit and H. P. J. Wijn, *Ferrites* (Wiley, New York, 1959), Chap. 8, pp. 136–175.

[24]J. P. Remeika and R. L. Comstock, J. Appl. Phys. **35**, 3320 (1964).

[25]G. A. Petrakovskii, V. N. Seleznev, K. A. Sablina, and L. M. Protopopova, Fiz. Tverd. Tela (Leningrad) **11**, 11 (1969) [Soy. Phys.—Solid State **11**, 7 (1969)].

[26]D. Wegner, Hyperfine Int. **23**, 179 (1985).

[27]H. Frauenfelder and R. M. Steffen, in *α-, β- and γ-Ray Spectroscopy,* edited by K. Siegbahn (North-Holland, Amsterdam, 1964), Vol. 2, p. 1111.

[28]K. Alder, E. Matthias, W. Schneider, and R. M. Steffen, Phys. Rev. **129**, 1199 (1963).

[29]M. J. L. Yates, in Ref. 27, p. 1691.

[30]K. Asai, F. Ambe, S. Ambe, and H. Sekizawa, J. Phys. Soc. Jpn. **53**, 4109 (1984).

[31]F. Ambe, K. Asai, S. Ambe, T. Okada, and H. Sekizawa, Hyperfine Int. **29**, 1197 (1986).

[32]K. Asai, F. Ambe, S. Ambe, T. Okada, and H. Sekizawa, Hyperfine Int. **34**, 277 (1987).

[33]The oxygen positions are described well by the oxygen parameter u even in $Li_{0.5}Fe_{2.5}O_4$. See Ref. 20.

[34]W. Gordy and W. J. O. Thomas, J. Chem. Phys. **24**, 439 (1956).

[35]L. Pauling, J. Am. Chem. Soc. **51**, 1010 (1929).

[36]W. H. Zachariasen, Acta Crystallogr. **16**, 385 (1963).

[37]I. D. Brown and R. D. Shannon, Acta Crystallogr. **A29**, 266 (1973).